

# Intensified East Asian summer monsoon and associated precipitation mode shift under the 1.5 °C global warming target

WANG Tao<sup>a,b,\*</sup>, MIAO Jia-Peng<sup>a,c</sup>, SUN Jian-Qi<sup>a,b,c</sup>, FU Yuan-Hai<sup>d</sup>

<sup>a</sup> Nansen-Zhu International Research Center, Institute of Atmospheric Physics, Chinese Academy of Sciences, Beijing 100029, China

<sup>b</sup> Collaborative Innovation Center on Forecast and Evaluation of Meteorological Disasters, Nanjing University of Information Science and Technology, Nanjing 210044, China

<sup>c</sup> University of Chinese Academy of Sciences, Beijing 100049, China

<sup>d</sup> Climate Change Research Center, Chinese Academy of Sciences, Beijing 100029, China

Received 25 September 2017; revised 11 December 2017; accepted 12 December 2017

Available online 19 December 2017

## Abstract

In this study, the East Asian summer climate changes under the 1.5 °C global warming (1.5 GW) target in 30 simulations derived from 15 coupled models within the Coupled Model Intercomparison Program phase 5 (CMIP5) are examined. Compared with the current summer climate (1975–2005), both surface air temperature and precipitation increase significantly over the East Asian continent during the 1.5 GW period (average period 2021–2051). In northeastern China this is particularly pronounced with regional averaged precipitation increases of more than 7.2%, which is greater than that for the whole East Asian continent (approximately 4.2%). Due to stronger enhancement of precipitation north of 40°N, the leading empirical orthogonal function (EOF) mode of summer precipitation over the East Asian continent changes from tripolar-like mode to dipole mode. As there is stronger surface warming over the East Asian continent than that over surrounding ocean, the land–sea thermal contrast is enhanced during the 1.5 GW period. As a result, the monsoon circulation in the lower troposphere is significantly strengthened, which causes the increased summer precipitation over the East Asian continent. In addition, larger interannual variabilities of East Asian summer monsoon circulation and associated precipitation are also suggested for the 1.5 GW period.

**Keywords:** East Asian summer monsoon; Precipitation; 1.5 °C global warming target; CMIP5

## 1. Introduction

The East Asian summer monsoon (EASM) is a subtropical monsoon system, whose domain includes eastern China, Korea, Japan, the adjacent marginal seas, and the South China Sea (Tao and Chen, 1987; Wang and Lin, 2002; Ding and Chan, 2005; Ding et al., 2007). It leads to heavy rainfall during summer and provides up to two-thirds of the annual

precipitation for most regions of East Asia (Ding, 1992; Gong and Ho, 2003). Therefore, the EASM has tremendous influences on water resources, agriculture and human society throughout East Asia.

The EASM and associated precipitation has large interannual variabilities. Usually, changes in EASM intensity lead to a position shift of the major monsoon rainfall belt, which can be affected by the El Niño–Southern Oscillation (ENSO) (Wang et al., 2000; Wang, 2002), Arctic sea ice (Guo et al., 2014), and some natural external forcings (Peng et al., 2010; Cui et al., 2014).

On an interdecadal timescale, significant weakening of the EASM was found in the late 1970s (Wang, 2001, 2002). This had associated monsoon precipitation increases in the Yangtze

\* Corresponding author. Nansen-Zhu International Research Center, Institute of Atmospheric Physics, Chinese Academy of Sciences, Beijing 100029, China.

E-mail address: [wangtao@mail.iap.ac.cn](mailto:wangtao@mail.iap.ac.cn) (WANG T.).

Peer review under responsibility of National Climate Center (China Meteorological Administration).

River Valley region and precipitation decreases in northern China, showing a named southern flood and northern drought pattern (Ding et al., 2008, 2009; Zhao et al., 2010). In addition, due to changes in background circulation, monsoon precipitation increases in the Huang-Huai region and decreases in the Yangtze River Valley from the end of 1990s have been observed (Zhu et al., 2011). As a result of these observations, the interdecadal variability of the EASM and its associated precipitation have become more prominent in the last 60 years (1950–2012) (Ding et al., 2015).

These interdecadal changes in EASM can be attributed to natural factors, such as the Pacific Decadal Oscillation (Qian and Zhou, 2014; Yu et al., 2015; Zhu et al., 2015) and the Atlantic Multidecadal Oscillation (Wang et al., 2009; Zhu et al., 2016). However, more evidence indicates the tremendous impact of anthropogenic forcings, including increased greenhouse gases emissions and anthropogenic aerosols, on the EASM and its associated precipitation (Mahmood and Li, 2012; Wang et al., 2013; Song et al., 2014). Therefore, more work is needed to detect the anthropogenic signal and related processes that are causing long-term changes of EASM. Understanding how the EASM and its associated precipitation respond to the expected global warming is especially critical in the 21st century.

In recent years, more attention has been paid to the projection of climate changes in East Asia (Jiang et al., 2004; Sun and Ding, 2010; Jiang and Tian, 2013). Based on multi model results from the Coupled Model Intercomparison Program phases 3 (CMIP3) and 5 (CMIP5), changes in temperature (e.g., Jiang et al., 2009; Xu et al., 2009; Chen et al., 2011; Wang et al., 2017a), precipitation (Gao et al., 2012; Chen and Sun, 2013; Niu et al., 2015; Wu et al., 2016), and their extremes (Chen et al., 2012; Jiang et al., 2012; Wang et al., 2012; Chen, 2013) by the middle and end of the 21st century, have been documented. As noted by Chen et al. (2011), summer temperature over China could increase by 3.7 °C by the end of the 21st century under the A1B scenario. Besides, a more pronounced increase in precipitation can be found over the Huang-Huai region, Shandong Peninsula and Northwest China (Gao et al., 2012). China could experience increased amounts of flooding due to more frequencies of heavy rainfall at the end of 21st century (Chen et al., 2012). In addition, an atlas was also created by Dong et al. (2012), which shows the substantive results from the CMIP5 experiments' data on climate changes over the next 100 years.

To prevent dangerous anthropogenic interference with the climate system, a 2 °C global warming target was used as a desirable temperature target in the Copenhagen Accord in 2009. Focusing on this target, possible climate changes over East Asia have been investigated (Sui et al., 2015; Jiang et al., 2016). In December 2015, the Paris Agreement agreed to pursue efforts to limit the temperature increase to 1.5 °C above pre-industrial levels. However, there is still a relative lack of scientific knowledge about the implications of 1.5 °C of global warming (hereafter abbreviated to 1.5 GW) (Hulme, 2016; Mitchell et al., 2016; Henley and King, 2017; Kong and Wang, 2017). Therefore, to find out what the possible

responses of EASM under the 1.5 GW target are, we investigate changes in the East Asian summer climate using CMIP5 multi model results.

In the remainder of this paper, Section 2 describes the models, data, and the method employed; Section 3 compares the simulated East Asian summer climate, including surface air temperature, precipitation and circulation, in the 1.5 GW period, with simulated current climate; Section 3 focuses on the potential mean climate and interannual variability changes; and conclusions are given in Section 4.

## 2. Model, data, and method

Two sets of simulations from 15 coupled models within CMIP5 are analyzed in this study (Taylor et al., 2012). The historical simulations are forced by both the anthropogenic forcings (greenhouse gases, anthropogenic aerosols, and land use) and natural forcings (total solar irradiance and volcanic aerosols). The 21st century simulations are run under the Representative Concentration Pathway (RCP) mid-low-range (RCP4.5) emission scenarios which are employed in this study. Details for the 15 CMIP5 coupled models adopted in this study can be found in Table 1. In addition, the observed precipitation data used in this study is from the Climatic Research Unit Time-Series Version 3.24.01 data set (UEACRU et al., 2017).

The timing of 1.5 GW for each model is based on 31-year running averages of the global mean temperature with reference to 1869–1899 (same method as Wang et al., 2017b). As shown in Table 1, the timing periods for 1.5 GW in these 15 CMIP5 coupled models are very different, implying the model-dependent responses of the climate system to possible further anthropogenic forcings. The average period for 1.5 GW is 2021–2051. To investigate the impacts associated with 1.5 GW, we mainly analyze the differences of the simulated East Asian summer (June–August) climate between the 31-year period centered at the timing of 1.5 GW and the current period (1975–2005). A standard *t*-test is applied here

Table 1  
Details of 15 CMIP5 coupled models and their periods to reach 1.5 GW.

Model	Institute	Atmospheric resolution	1.5 GW period
bcc-csm1-1	BCC/China	64 × 128	2008–2038
CNRM-CM5	CNRM-CERFACS/France	128 × 256	2023–2053
CSIRO-Mk3-6-0	CSIRO-QCCCE/Australia	96 × 192	2020–2050
FGOALS-g2	IAP-THU/China	60 × 128	2024–2054
GFDL-CM3	NOAA-GFDL/USA	90 × 144	2009–2039
GFDL-ESM2G	NOAA-GFDL/USA	90 × 144	2039–2069
GFDL-ESM2M	NOAA-GFDL/USA	90 × 144	2031–2061
GISS-E2-H	NASA-GISS/USA	90 × 144	2009–2039
GISS-E2-R	NASA-GISS/USA	90 × 144	2028–2058
HadGEM2-CC	MOHC/UK	145 × 192	2021–2051
HadGEM2-ES	MOHC/UK	145 × 192	2014–2044
MIROC5	MIROC/Japan	128 × 256	2025–2055
MIROC-ESM-CHEM	MIROC/Japan	64 × 128	2007–2037
MRI-CGCM3	MRI/Japan	160 × 320	2040–2070
NorESM1-M	NCC/Norway	96 × 144	2026–2056

to determine their significance level. In addition to the single model analysis, the multi model ensemble (MME) results are also analyzed in this study.

The empirical orthogonal function (EOF) analysis is used to investigate the shifting of the summer precipitation pattern over the East Asian continent during the 1.5 GW period. To examine the changes in intensity of EASM circulation, we use the EASM index defined as area-mean velocity at 850 hPa over the region of 110°–125°E, 20°–40°N (Wang, 2002).

### 3. Results

#### 3.1. Surface air temperature and precipitation

During the 1.5 GW period, surface air temperature increases significantly over the East Asian region (Fig. 1). In the continental areas the surface air warming is stronger than that over the surrounding ocean. Such surface warming characteristics are captured by all models employed. In addition, the MME indicates that the warming maximums are located in western China. For the East Asian continent and the northwestern Pacific Ocean, surface air warming becomes stronger with increasing latitude. In addition, the magnitude of

terrestrial warming is generally greater when compared with warming over the ocean at same latitude.

At the same time, summer precipitation is also enhanced over most regions of East Asia (Fig. 2). Most models simulate increased summer precipitation over the Qinghai–Tibetan Plateau and higher-latitude regions, although the inter-model discrepancies are very large. CNRM-CM5, GISS-E2-R, and MRI-CGCM3 simulate significantly decreased summer precipitation in the Yangtze River Valley. The MME suggests summer precipitation increased over most of the East Asian continental regions except for southeastern China. In addition, the maximum positive anomalies for summer precipitation are located over northeastern China and the Qinghai–Tibetan Plateau. Compared with the current climate, the summer precipitation increases by approximately 10% over these regions (Fig. 3). For the northern part of the Indo–China Peninsula, the summer precipitation also increases by 5%.

Statistical analysis showed that regional averaged summer precipitation over the East Asian continent (20°–50°N, 80°–140°E) will increase by ~1% to ~7%, depending on the model used, during the 1.5 GW period (Fig. 4). The mean increase is more than 4.2%. In contrast, most models simulate a larger increase in averaged summer precipitation over Northeast

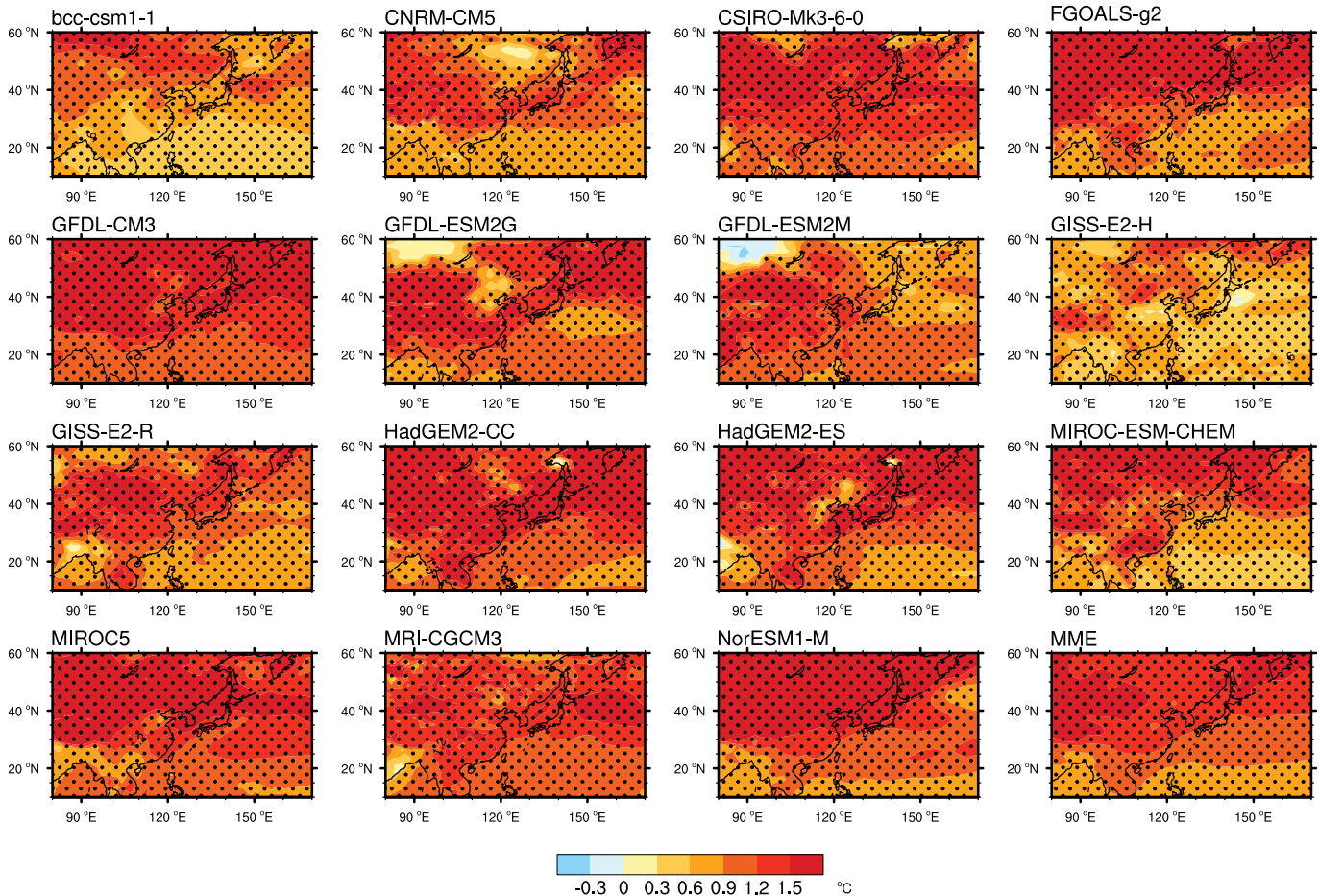


Fig. 1. Simulated differences between a 1.5 GW rise and the current climate (1.5 GW – current) in summer surface air temperature (Areas with confidence level exceeding 95% are denoted with dots).

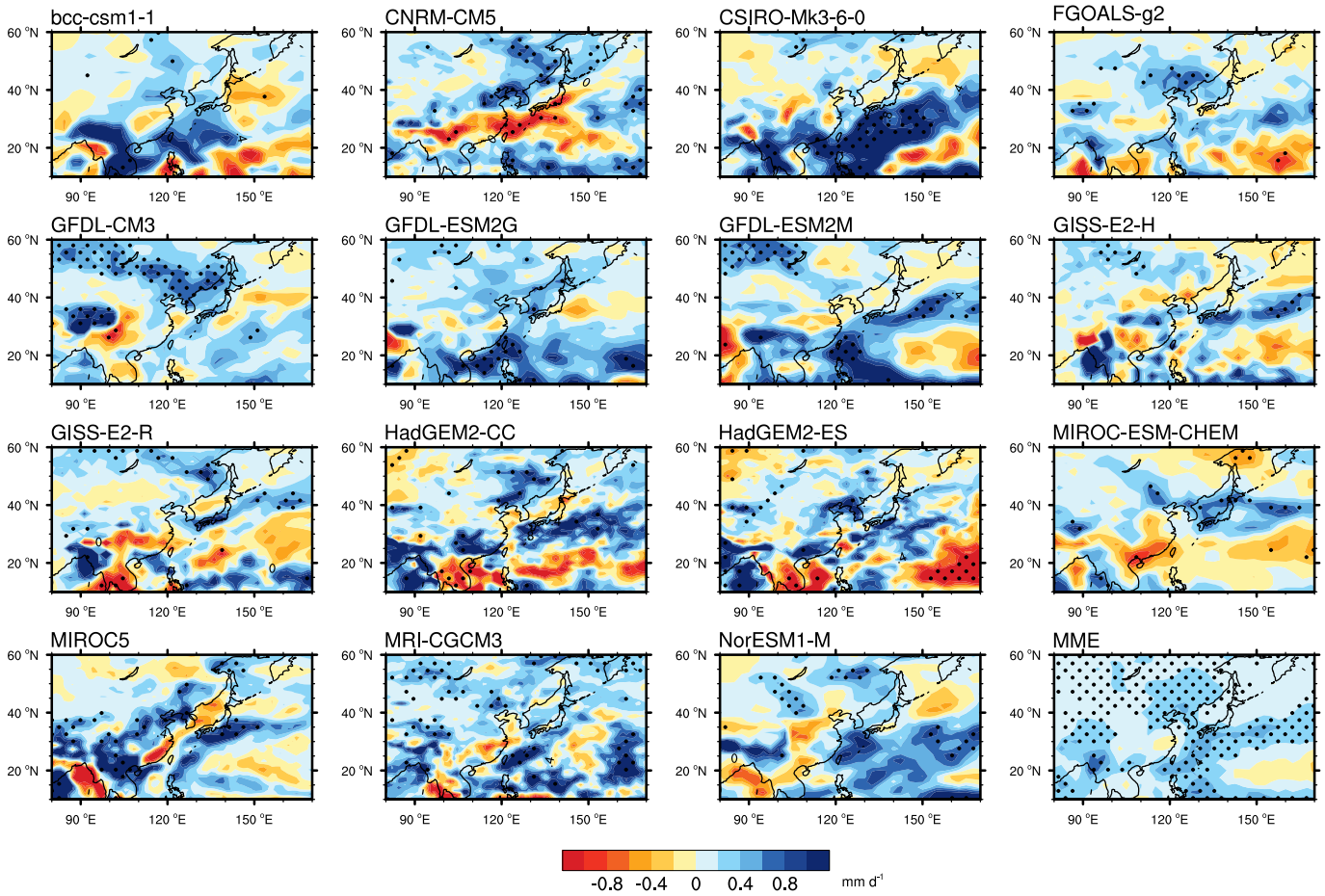


Fig. 2. Simulated differences (1.5 GW – current) in summer precipitation (Areas with confidence level exceeding 95% are denoted with dots).

China (40°–55°N, 120°–140°E). The CNRM-CM5, GFDL-CM3, and HadGEM2-CC models showed that the regional averaged precipitation will increase by more than 10%. The mean value of all the models reaches up to 7.2%, higher than the value for the whole East Asian continent.

Due to stronger increase in summer precipitation north of 40°N, the main EOF modes of summer precipitation

anomalies over the East Asian continent shift during the 1.5 GW period. As shown in Fig. 5a, the leading EOF mode in the observation is a tripolar-like precipitation anomaly pattern with positive anomalies in the Yangtze River Valley and negative anomalies over northern and southern China. Its

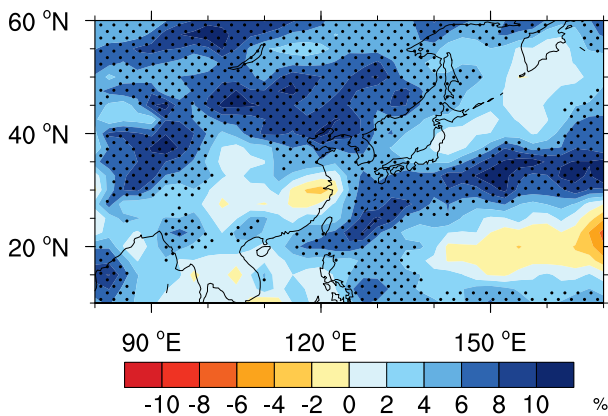


Fig. 3. Simulated changes  $((1.5 \text{ GW} - \text{current})/\text{current} \times 100\%)$  in summer precipitation (Areas with confidence level exceeding 95% are denoted with dots).

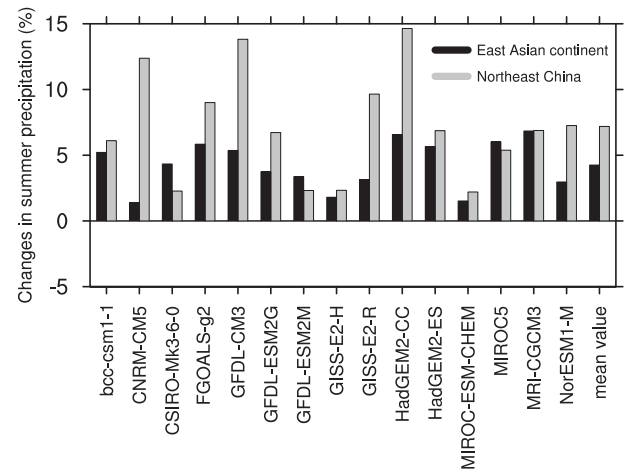


Fig. 4. Simulated changes  $((1.5 \text{ GW} - \text{current})/\text{current} \times 100\%)$  in regional averaged summer precipitation (unit: %) for the East Asian continent (20°–50°N, 80°–140°E) and Northeast China (40°–55°N, 120°–140°E).

explained variance is 19.0%. The observed second EOF mode is a dipole precipitation anomaly pattern, demonstrating reverse precipitation anomalies over northern and southern parts of China (Fig. 5b). Here, the explained variance is 14.8%, slightly less than the leading mode. The MME for the current climate reproduces similar leading and second EOF modes of summer precipitation anomaly patterns in the observation (Fig. 5c and d). Their explained variances are also close to the observed values. This suggests that the MME can

capture the distribution characteristics of observed precipitation over the East Asian continent. For the 1.5 GW period, the MME simulates different EOF modes. The leading EOF mode is replaced by the dipole precipitation anomaly pattern (Fig. 5e), which is the second EOF mode in the current climate. Its explained variance reaches up to 26%, increasing by more than 10% and implying a significant raised likelihood of a north–south distribution of summer precipitation over the East Asian continent north of 40°N in the 1.5 GW period. The

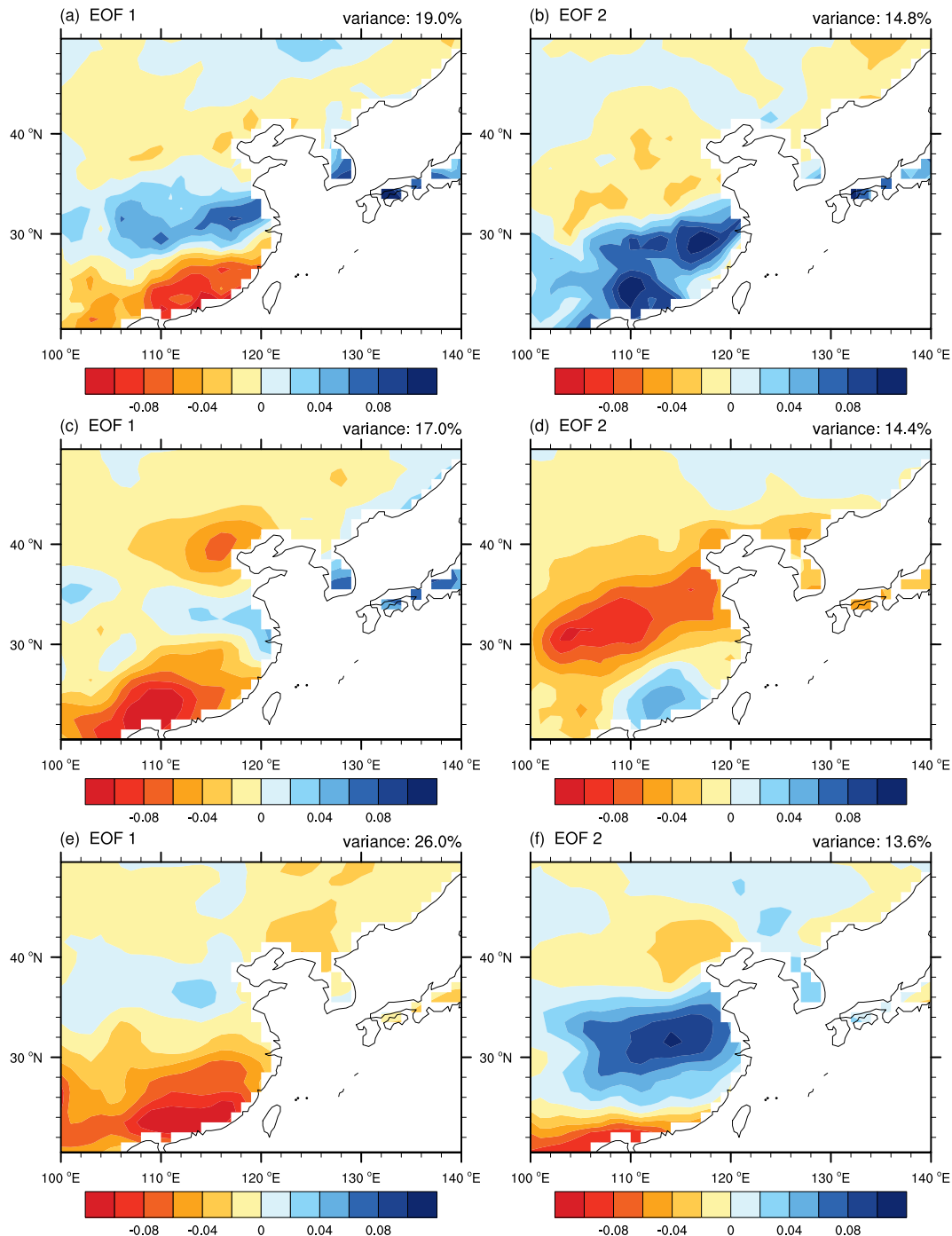


Fig. 5. Leading and second EOF modes of anomalous summer precipitation in the observed (a, b), CMIP5 current climate (c, d), and CMIP5 1.5 GW period (e, f).

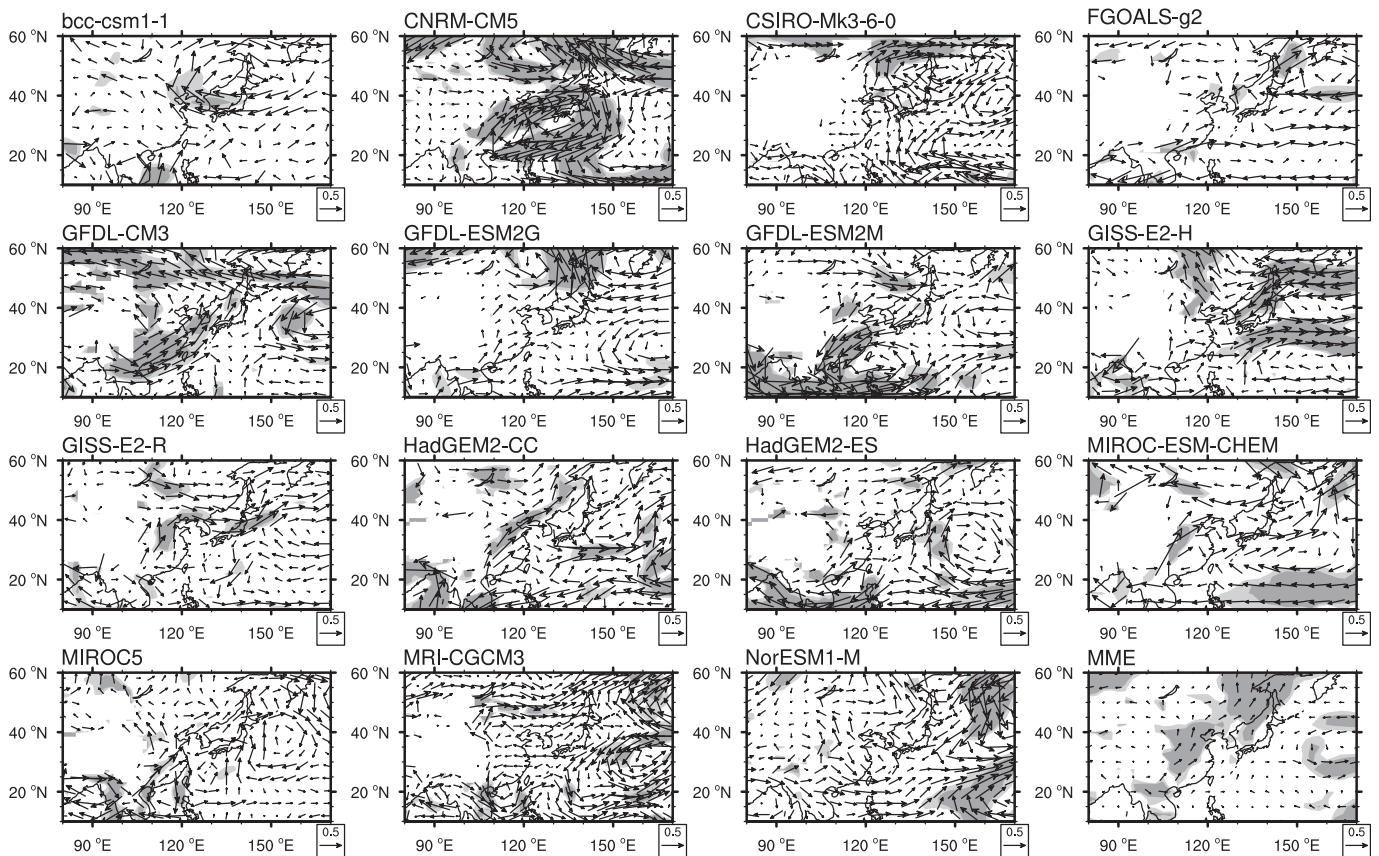


Fig. 6. Simulated differences ( $1.5 \text{ GW} - \text{current}$ ) in summer wind fields at  $850 \text{ hPa}$  (unit:  $\text{m s}^{-1}$ ). Areas with confidence level exceeding 90%/95% are shaded with light/gray.

tripolar-like precipitation anomaly pattern becomes the second EOF mode and its explained variance is lowered to 13.6% (Fig. 5f).

### 3.2. Monsoon circulation

Changes in EASM circulation is the main factor causing precipitation anomalies in East Asia. Most models simulate a stronger EASM circulation for the 1.5 GW period (Fig. 6). Southerly wind anomalies can be seen over the East Asian continent. Some differences between the models also exist. For example, the GFDL-ESM2M and MRI-CGCM3 models simulate northerly wind anomalies over southern China, whereas the MME shows significantly strengthened summer monsoon circulation over most regions of the East Asian continent. Therefore, the rainfall belt shifts more northward and summer precipitation increases over northern China, especially over northeastern China during the 1.5 GW period. Additionally, anomalously cyclonic circulation can be found over the northwestern Pacific. Together with C-shape positive summer precipitation anomalies there (Fig. 3, MME), this anomalously cyclonic circulation suggests that the location of the western Pacific subtropical high will be more east when compared with the current climate.

Due to stronger surface warming over the East Asian continent compared with the surrounding ocean, as mentioned

above, most models simulate negative sea level pressure (SLP) anomalies over the continental regions and positive SLP over the northwestern Pacific (Fig. 7). Although there are some differences in the distribution and magnitude of the SLP anomalies, enhanced land–sea thermal contrast can be found in these models and cause stronger EASM circulation during the 1.5 GW period. On the contrary, GFDL-ESM2M and MRI-CGCM3 simulate negative SLP anomalies over the northwestern Pacific and weak positive SLP anomalies over some continental regions. Thus, the land–sea thermal contrast is reduced, which explains the emergence of northerly wind anomalies over southern China in these two models.

On the average, significant negative SLP anomalies are evident over northwestern China and west of Lake Baikal in the MME (Fig. 7). At the same time, significant positive SLP anomalies can be found over the Qinghai–Tibetan Plateau, the Indo–China Peninsula, and tropical northwestern Pacific. This SLP anomaly pattern indicates an increased south–north land–sea thermal contrast and can result in the strengthened summer monsoon circulation in the lower troposphere.

In the upper troposphere, changes in the East Asia westerly jet (EAJ) are very different between models during the 1.5 GW period (Fig. 8). CSIRO-Mk3-6-0, FGOALS-g2, GFDL-ESM2G, GFDL-ESM2M, and MRI-CGCM3 simulate a stronger EAJ. Yet, CNRM-CM5 and GISS-E2-R simulate a weakened and northward shifted EAJ. MIROC-ESM-CHEM

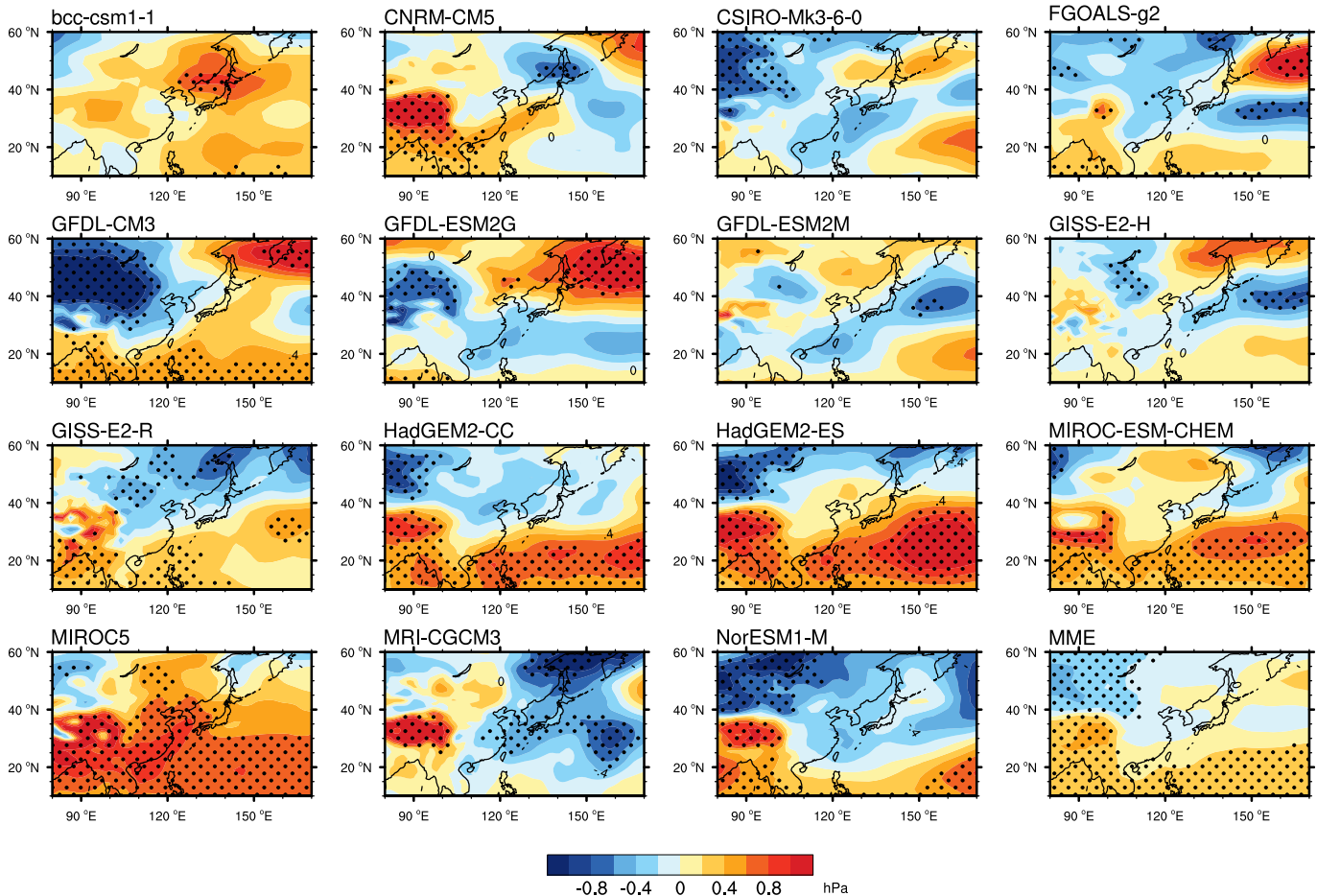


Fig. 7. Simulated differences (1.5 GW – current) in summer sea level pressure (Areas with confidence level exceeding 95% are denoted with dots).

simulates a significantly weakened EAJ. Other models do not simulate significant changes in EAJ during the 1.5 GW period. For the MME, positive westerly wind anomalies can be found only over the entrance of the EAJ (Fig. 8, MME). Associated secondary circulation can cause enhanced ascending motion, which explains the increased precipitation over the Qinghai–Tibetan Plateau and southern part of the Indo–China Peninsula (Fig. 3).

### 3.3. Interannual variability of the EASM

The interannual variability of EASM responses to the 1.5 GW is a very important issue. Compared with the current climate, changes of standard deviations of the EASM index for the 1.5 GW period vary among models and ranging from 40.1% (GFDL-ESM2G) to –34.7% (MRI-CGCM3) (Fig. 9). Their mean value is very small, ~2%. Standard deviations from four models (GFDL-CM3, GFDL-ESM2M, HadGEM2-CC, and MRI-CGCM3) decrease by more than 10% when compared with the current climate. However, standard deviations from seven models (bcc-csm1-1, FGOALS-g2, GFDL-ESM2G, GISS-E2-R, HadGEM2-ES, MIROC-ESM-CHEM, and MIROC5) increase by more than 10%. This

suggests that interannual variability of the EASM circulation is likely to be larger in the 1.5 GW period than in the current climate.

For the regional averaged summer precipitation over the East Asian continent and Northeast China, the mean values of their standard deviations increase by 12.2% and 14.5%, respectively, during the 1.5 GW period relative to the current climate (Fig. 10). Consistent responses are found in most of the models suggesting that the interannual variability of the terrestrial summer precipitation over East Asia is also enhanced during the 1.5 GW period.

## 4. Conclusions and discussion

In this study, to investigate responses of East Asian summer climate under 1.5 GW target, the multi model results from CMIP5 were analyzed. Results showed that both surface air temperature and precipitation significantly increase over most regions of East Asia during the 1.5 GW period (average period 2021–2051 based on the 15 CMIP5 coupled models). Compared with the current climate, regional averaged summer precipitation is projected to increase by about 7.2% over Northeast China, which is higher than the increase predicted

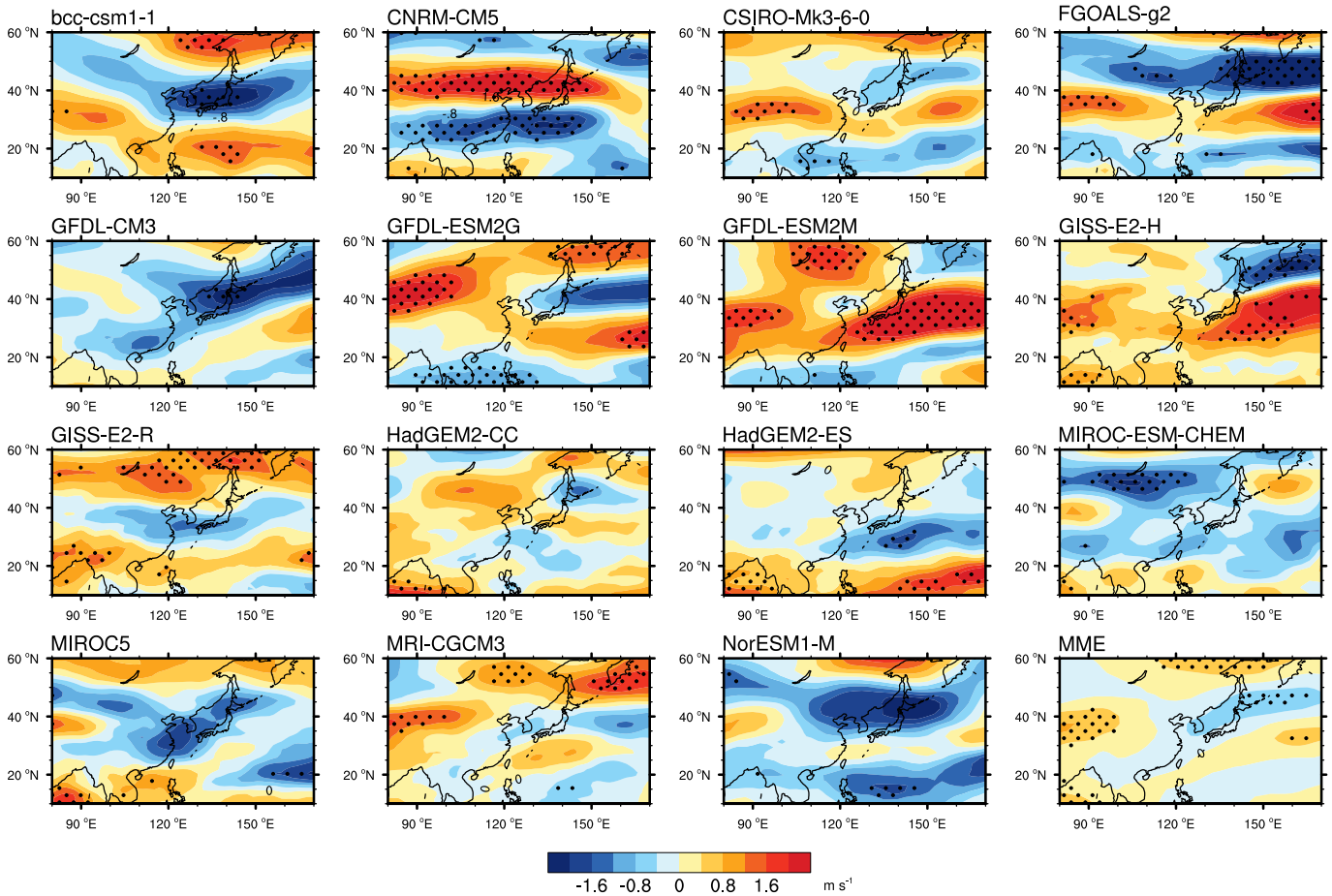


Fig. 8. Simulated differences (1.5 GW – Current) in summer zonal wind at 200 hPa. Areas with confidence level exceeding 95% are denoted with dots.

for the entire East Asian continent (4.2%). Due to higher precipitation north of 40°N, the leading EOF mode for the East Asian summer precipitation changes from a tripolar-like mode to a dipole mode, suggesting higher frequencies of north–south precipitation anomaly distribution in the near future.

During the 1.5 GW period, increased summer precipitation and possible precipitation mode shift are closely linked to changes of EASM circulation. Due to stronger warming over the East Asian continent compared with the surrounding ocean, the land–sea thermal contrast is enhanced. As a result,

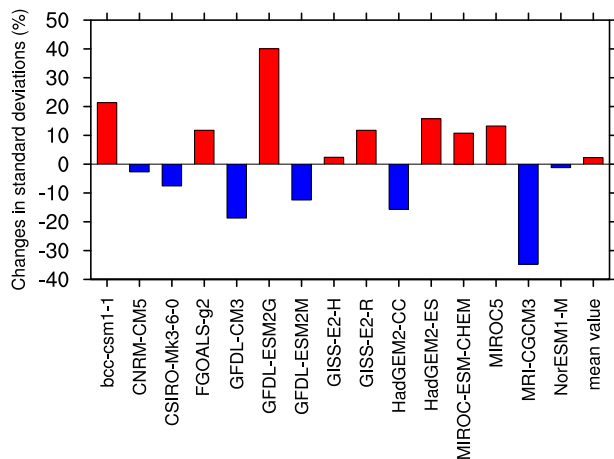


Fig. 9. Simulated changes ((1.5 GW – current)/current × 100%) in standard deviations of the EASM index.

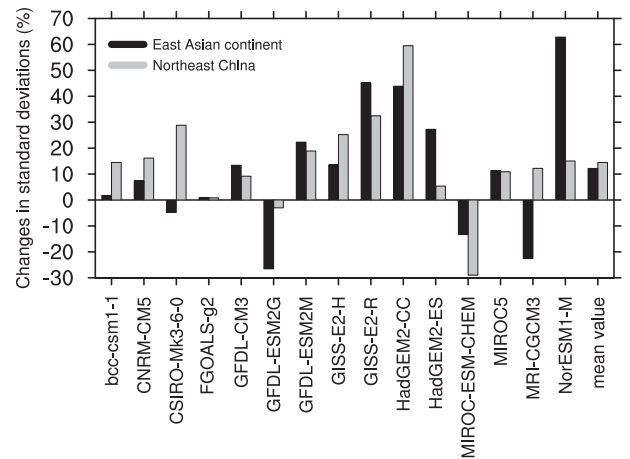


Fig. 10. Simulated changes ((1.5 GW – current)/current × 100%) in standard deviations of regional averaged summer precipitation for the East Asian continent (20–50°N, 80–140°E) and northeastern China (40–55°N, 120–140°E).

southerly wind anomalies are evident over East Asia in the results of MME and most other models. The monsoon circulation in the lower troposphere is significantly strengthened. This mainly contributes to the increased summer precipitation over East Asia, particularly for regions north of 40°N. However, the EAJ does not show a significant response to the 1.5 GW rise. In addition, larger interannual variabilities of EASM circulation and associated precipitation are also suggested to occur during the 1.5 GW period.

During the 1.5 GW period, the regional averaged surface air temperature over the East Asia increases by about 2 °C. This is lower than that over North Asia (~2.7 °C), further confirming stronger temperature rises at higher latitudes than at lower latitudes (Xu et al., 2017). Change in summer precipitation over the East Asia is also smaller than that over the North Asia (~9%). From the 1.5 GW period to the 2 °C global warming period, summer precipitation changes little over the East Asia, whereas the surface air temperature increase by more than 0.5 °C (Xu et al., 2017). It suggests a faster warming over the East Asian continent than the global averaged.

In the CMIP5, there are four different RCP emissions scenarios (RCP2.6, RCP4.5, RCP6.0, and RCP8.5). For the different RCP emissions scenarios, the timing periods to reach 1.5 GW are very different. The stronger the RCP emissions scenario, the earlier we will reach the period of 1.5 GW. However, based on some preliminary analysis, spatial distributions of differences in mean climate (e.g., temperature and precipitation) between a long-term 1.5 GW period (e.g., longer than 31-year climatology) and pre-industrial are almost the same in different RCP emissions scenarios, particularly for the MME. In this study, therefore, only the simulations under the mid-low-range RCP scenario (i.e., RCP 4.5) are employed. However, a sufficient analysis of the output from all the RCP emissions scenarios is necessary and will be complete in the future.

## Acknowledgments

This research was supported by the National Key R&D Program of China (2017YFA0603802), the National Natural Science Foundation of China (41661144005 and 41320104007), and the CAS–PKU Joint Research Program. We would like to thank the IPCC for providing the CMIP5 datasets ([http://www.ipcc-data.org/sim/gcm\\_monthly/AR5/Reference-Archive.html](http://www.ipcc-data.org/sim/gcm_monthly/AR5/Reference-Archive.html)).

## References

- Chen, H.P., 2013. Projected change in extreme rainfall events in China by the end of the 21st century using CMIP5 models. *Chin. Sci. Bull.* 58, 1462–1472.
- Chen, H.P., Sun, J.Q., 2013. Projected change in East Asian summer monsoon precipitation under RCP scenario. *Meteorol. Atmos. Phys.* 121, 55–77.
- Chen, H.P., Sun, J.Q., Chen, X.L., et al., 2012. CGCM projections of heavy rainfall events in China. *Int. J. Climatol.* 32, 441–450.
- Chen, W.L., Jiang, Z.H., Li, L., 2011. Probabilistic projections of climate change over China under the SRES A1B scenario using 28 AOGCMs. *J. Clim.* 24, 4741–4756.
- Cui, X.D., Gao, Y.Q., Sun, J.Q., 2014. The response of the East Asian summer monsoon to strong tropical volcanic eruptions. *Adv. Atmos. Sci.* 31, 1245–1255.
- Ding, Y.H., 1992. Summer monsoon rainfalls in China. *J. Meteorol. Soc. Jpn.* 70, 373–396.
- Ding, Y.H., Chan, J.C.L., 2005. The East Asian summer monsoon: an overview. *Meteorol. Atmos. Phys.* 89, 117–142.
- Ding, Y.H., Wang, Z.Y., Sun, Y., 2008. Inter-decadal variation of the summer precipitation in East China and its association with decreasing Asian summer monsoon. Part I: observed evidences. *Int. J. Climatol.* 28, 1139–1161.
- Ding, Y.H., Liu, Y.J., Song, Y.F., et al., 2015. From MONEX to the global monsoon: a review of monsoon system research. *Adv. Atmos. Sci.* 32, 10–31.
- Ding, Y.H., Sun, Y., Wang, Z.Y., et al., 2009. Inter-decadal variation of the summer precipitation in China and its association with decreasing Asian summer monsoon part II: possible causes. *Int. J. Climatol.* 29, 1926–1944.
- Ding, Y.H., Ren, G.Y., Zhao, Z.C., et al., 2007. Detection, causes and projection of climate change over China: an overview of recent progress. *Adv. Atmos. Sci.* 24, 954–971.
- Dong, W.J., Ren, F.M., Huang, J.B., et al., 2012. The atlas of climate change: based on SEAP-CMIP5. <https://doi.org/10.1007/978-3-642-31773-6>. Springer Sciences and Business Media, GX Dordrecht.
- Gao, X.J., Shi, Y., Zhang, D.F., et al., 2012. Uncertainties in monsoon precipitation projections over China: results from two high-resolution RCM simulations. *Clim. Res.* 52, 213–226.
- Gong, D.Y., Ho, C.H., 2003. Arctic oscillation signals in the East Asian summer monsoon. *J. Geophys. Res. Atmos.* 108, 4066.
- Guo, D., Gao, Y.Q., Bethke, I., et al., 2014. Mechanism on how the spring Arctic sea ice impacts the East Asian summer monsoon. *Theor. Appl. Climatol.* 115, 107–119.
- Henley, B.J., King, A.D., 2017. Trajectories toward the 1.5° C Paris target: modulation by the interdecadal Pacific oscillation. *Geophys. Res. Lett.* 44, 4256–4262.
- Hulme, M., 2016. 1.5° C and climate research after the Paris agreement. *Nat. Clim. Change* 6, 222–224.
- Jiang, D.B., Tian, Z.P., 2013. East Asian monsoon change for the 21st century: results of CMIP3 and CMIP5 models. *Chin. Sci. Bull.* 58, 1427–1435.
- Jiang, D.B., Wang, H.J., Lang, X.M., 2004. East Asian climate change trend under global warming background. *Chin. J. Geophys. – Chin. Edn.* 47, 590–596.
- Jiang, D.B., Sui, Y., Lang, X.M., 2016. Timing and associated climate change of a 2° C global warming. *Int. J. Climatol.* 36, 4512–4522.
- Jiang, D.D., Zhang, Y., Sun, J.Q., 2009. Ensemble projection of 1–3° C warming in China. *Chin. Sci. Bull.* 54, 3326–3334.
- Jiang, Z.H., Song, J., Li, L., et al., 2012. Extreme climate events in China: IPCC-AR4 model evaluation and projection. *Clim. Change* 110, 385–401.
- Kong, Y., Wang, C.H., 2017. Responses and changes in the permafrost and snow water equivalent in the Northern Hemisphere under a scenario of 1.5° C warming. *Adv. Clim. Change Res.* 8 (4), 235–244.
- Mahmood, R., Li, S.L., 2012. Response of summer rainfalls in Pakistan to dust aerosols in an atmospheric general circulation model. *Idojaras* 116, 323–335.
- Mitchell, D., James, R., Forster, P.M., et al., 2016. Realizing the impacts of a 1.5° C warmer world. *Nat. Clim. Change* 6, 735–737.
- Niu, X.R., Wang, S.Y., Tang, J.P., et al., 2015. Multimodel ensemble projection of precipitation in eastern China under A1B emission scenario. *J. Geophys. Res. Atmos.* 120, 9965–9980.
- Peng, Y.B., Shen, C.M., Wang, W.C., et al., 2010. Response of summer precipitation over eastern China to large volcanic eruptions. *J. Clim.* 23, 818–824.
- Qian, C., Zhou, T.J., 2014. Multidecadal variability of north China aridity and its relationship to PDO during 1900–2010. *J. Clim.* 27, 1210–1222.
- Song, F.F., Zhou, T.J., Qian, Y., 2014. Responses of East Asian summer monsoon to natural and anthropogenic forcings in the 17 latest CMIP5 models. *Geophys. Res. Lett.* 41, 596–603.
- Sui, Y., Lang, X.M., Jiang, D.B., 2015. Temperature and precipitation signals over China with a 2° C global warming. *Clim. Res.* 64, 227–242.
- Sun, Y., Ding, Y.H., 2010. A projection of future changes in summer precipitation and monsoon in East Asia. *Sci. China Earth Sci.* 53, 284–300.
- Tao, S.Y., Chen, L., 1987. A review of recent research on the East Asian summer monsoon in China. In: Chang, C.P., Krishnamurti, T.N. (Eds.), *Monsoon Meteorology*. Oxford University Press, pp. 60–92.

- Taylor, K.E., Stouffer, R.J., Meehl, G.A., 2012. An overview of Cmp5 and the experiment design. *Bull. Am. Meteorol. Soc.* 93, 485–498.
- UEACRU (University of East Anglia Climatic Research Unit), Harris, I.C., Jones, P.D., 2017. CRU TS3.24.01: climatic research unit (CRU) time-series (TS) Version 3.24.01 of high resolution gridded data of month-by-month variation in climate (Jan. 1901–Dec. 2015). *Cent. Environ. Data Anal.* <https://doi.org/10.5285/3df7562727314bab963282e6a0284f24>, 25 August 2017.
- Wang, B., Lin, Ho, 2002. Rainy season of the Asian-Pacific summer monsoon. *J. Clim.* 15, 386–398.
- Wang, B., Wu, R.G., Fu, X.H., 2000. Pacific-East Asian teleconnection: how does ENSO affect East Asian climate? *J. Clim.* 13, 1517–1536.
- Wang, G.J., Cai, W.J., Gan, B.L., et al., 2017b. Continued increase of extreme El Nino frequency long after 1.5° C warming stabilization. *Nat. Clim. Change* 7, 568–572.
- Wang, H.J., 2001. The weakening of the Asian monsoon circulation after the end of 1970s. *Adv. Atmos. Sci.* 18, 376–386.
- Wang, H.J., 2002. The instability of the East Asian summer monsoon – ENSO relations. *Adv. Atmos. Sci.* 19, 1–11.
- Wang, H.J., Sun, J.Q., Chen, H.P., et al., 2012. Extreme climate in China: facts, simulation and projection. *Meteorol. Z.* 21, 279–304.
- Wang, T., Wang, H.J., Ottera, O.H., et al., 2013. Anthropogenic agent implicated as a prime driver of shift in precipitation in eastern China in the late 1970s. *Atmos. Chem. Phys.* 13, 12433–12450.
- Wang, Y.J., Zhou, B.T., Qin, D.H., et al., 2017a. Changes in mean and extreme temperature and precipitation over the Arid region of northwestern China: observation and projection. *Adv. Atmos. Sci.* 34, 289–305.
- Wang, Y.M., Li, S.L., Luo, D.H., 2009. Seasonal response of Asian monsoonal climate to the Atlantic multidecadal oscillation. *J. Geophys. Res. Atmos.* 114, D02112.
- Wu, D., Jiang, Z.H., Ma, T.T., 2016. Projection of summer precipitation over the Yangtze-Huaihe River basin using multimodel statistical downscaling based on canonical correlation analysis. *J. Meteorol. Res.-Pr* 30, 867–880.
- Xu, Y., Gao, X.J., Giorgi, F., 2009. Regional variability of climate change hot-spots in East Asia. *Adv. Atmos. Sci.* 26, 783–792.
- Xu, Y., Zhou, B.T., Wu, J., Han, Z.Y., et al., 2017. Asian climate change under 1.5-4C warming targets. *Adv. Clim. Change Res.* 8, 99–107.
- Yu, L., Furevik, T., Ottera, O.H., et al., 2015. Modulation of the Pacific decadal oscillation on the summer precipitation over East China: a comparison of observations to 600-years control run of Bergen climate model. *Clim. Dynam.* 44, 475–494.
- Zhao, P., Yang, S., Yu, R.C., 2010. Long-term changes in rainfall over eastern China and large-scale atmospheric circulation associated with recent global warming. *J. Clim.* 23, 1544–1562.
- Zhu, Y.L., Wang, T., Ma, J.H., 2016. Influence of Internal decadal variability on the summer rainfall in eastern China as simulated by CCSM4. *Adv. Atmos. Sci.* 33, 706–714.
- Zhu, Y.L., Wang, H.J., Zhou, W., et al., 2011. Recent changes in the summer precipitation pattern in East China and the background circulation. *Clim. Dynam.* 36, 1463–1473.
- Zhu, Y.L., Wang, H.J., Ma, J.H., et al., 2015. Contribution of the phase transition of Pacific Decadal Oscillation to the late 1990s' shift in East China summer rainfall. *J. Geophys. Res. Atmos.* 120, 8817–8827.